THE JOURNAL OF VISUALIZATION AND COMPUTER ANIMATION
J. Visual. Comput. Animat. **9**, 53–63 (1998)

Tighter Error Bounds and Weighted Error Metrics for Hierarchical Radiosity

chin-chen chang and zen-chung shih*
Department of Computer and Information Science, National Chiao Tung University, Hsinchu, Taiwan 30010, Republic of China

SUMMARY

In this paper we first derive a tighter error bound on form factors as a subdivision criterion for the hierarchical radiosity algorithm. Such an error bound can reduce more unnecessary links and improve the performance of the hierarchical radiosity algorithm to meet a user-specified error tolerance. We then propose a weighted error metric in form factor computation such that more effort is automatically applied to shadow boundaries. Evaluating form factors along shadow boundaries with a higher degree of precision should enhance the quality of human perception. Using the proposed tighter error bound on the weighted error metric, we not only improve the performance but also increase the accuracy of the hierarchical radiosity algorithm. © 1998 John Wiley & Sons, Ltd.

key words: global illumination; error analysis; radiosity; visibility; shadow

1. INTRODUCTION

Radiosity provides a solution for the global illumination problem within a closed environment consisting of ideal diffuse reflectors and emitters. Radiosity approaches can only produce approximate results, thereby accounting for the existence of errors in the radiosity solution. If the error bound is too conservative, it will cause more unnecessary subdivisions in the radiosity algorithm to meet a user-specified error tolerance. Thus the computational cost becomes very expensive. Moreover, if the error is large, it will cause unacceptable radiosity soolutions. Therefore reliable error bounds and accurate error estimations are important for radiosity.

Up to now there have been several works devoted to the bound and error estimate for radiosity. Cohen *et al*.[1] proposed a two-level hierarchy known as the *substructuring technique* for radiosity. The patches, e.g. those along shadow boundaries, that exhibit a high radiosity gradient are subdivided further to yield accurate solutions. Hanrahan *et al*.[2] generalized the two-level hierarchy to a *multilevel hierarchy* from Appel's algorithm for resolving the *N*-body problem.[3] They computed an approximate

* Correspondence to: Zen-Chung Shih, Department of Computer and Information Science, National Chiao Tung University, Hsinchu, Taiwan 30010, Republic of China.
E-mail: zcshih@cc.nctu.edu.tw

CCC 1049–8907/98/020053–11$17.50

Received 31 May 1996
Revised 17 July 1997 and 23 Sept 1997

upper bound on the form factor and used a brightness-weighted refinement strategy as a criterion for determining the level in the hierarchy at which two patches can interact. Smits *et al.*[4] proposed an *importance-driven* radiosity approach that efficiently computes the view-dependent global solutions. Their algorithm refines any interaction if its estimated error exceeds the given error tolerance. Smits *et al.*[5] presented an algorithm for accelerating the hierarchical radiosity in complex environments by clustering objects. They used bounds on the potential error to transfer energy between objects. Arvo *et al.*[6] characterized possible sources of error in global illumination and derived bounds for each distinct category. To obtain better solutions, each source of an error should be considered. Lischinski *et al.*[7] proposed an approach to determine *a posteriori* bounds and estimates for local and total error of radiosity. Their algorithm considered the propagation of errors due to interreflections and provided conservative error bounds. Pellegrini[8] introduced a new characterization of form factors based on concepts from integral geometry. He proposed a new Monte Carlo algorithm to compute approximations of form factors with an error bounded *a priori* in an occluded polyhedral environment. Sillion and Drettakis[9] proposed a *feature-based error metric* for radiosity. They introduced an approach to controlling error in hierarchical clustering algorithms.

The shadow provides an important cue for human perception of image quality. An inaccurate evaluation of the visibility leads to errors in the shadow and subsequently affects the image quality. Owing to these reasons, the shadow should be accurately dealt with. To compute shadows efficiently and accurately, several approaches have been proposed.[10–15] However, most available methods are empirical and do not consider the reflection model. In fact, a Watt and Watt[16] indicate, the shadow is a local decrement in diffuse light because of the blocking of direct illumination. Shadows can be incorporated into the radiosity method because they are part of the diffuse interaction problem.

In this paper we first derive a better error bound for the hierarchical radiosity algorithm, that differs from the usual bound by a factor of $\frac{1}{2}$. Such an error bound can reduce more unnecessary links and improve the performance of the hierarchical radiosity algorithm to meet a user-specified error tolerance. However, this approach will decrease the accuracy of the shadow and thus affect the user's perception of image quality. Therefore we propose a weighted error metric in form factor computation to increase the accuracy of radiosity along shadow boundaries and penumbras. We define a weighting function in this metric, in which different areas may have different weights. Shadow boundaries may obtain more weights than others. Radiosities along shadow boundaries are computed with a higher degree of precision, while those of others are computed normally. Using our proposed tighter error bound on the weighted error metric, we improve the performance and enhance the accuracy of the hierarchical radiosity algorithm.

The rest of this paper is organized as follows. In Section 2 we derive a tighter error bound on form factors. In Section 3 we discuss the weighted error metric in form factor computation. Analysis and comparison are displayed in Section 4. Finally, conclusions and future work are given in Section 5.

2. TIGHTER ERROR BOUNDS ON FORM FACTORS

The form factor from a point x on patch P_i to patch P_j is given by the area integral with the kernel function $k(x,y)$,

$$F_{ij} = \int_{y \in P_j} k(x,y)\mathrm{d}y$$

where y is a point on P_j, and

$$k(x,y) = \frac{\cos\theta_i \cos\theta_j}{\pi r^2} v(x,y)$$

where r is the distance between x and y; θ_i is the angle formed by the normal of the differential area at x and the line connecting x and y; θ_j is the angle formed by the normal of the differential area at y and the line connecting x and y; and $v(x,y)$ is the visibility function, which is one if x and y are mutually visible, and zero otherwise.

We follow the notation of Smits *et al.*[5] in computing the form factor bounds. Let the maximum, minimum and average values of a function f over the domain $A \times B$ be defined by

$$\lceil f \rceil_{A,B} \equiv \max_{x \in A, y \in B} f(x,y)$$
$$\lfloor f \rfloor_{A,B} \equiv \min_{x \in A, y \in B} f(x,y)$$

and

$$\langle f \rangle_{A.B} \equiv \operatorname{avg}_{x \in A, y \in B} f(x,y)$$

respectively. The approximate form factor $\hat{F}_{ij}$ is given by

$$\hat{F}_{ij} = \langle k \rangle_{A,B} \cdot A_j$$

where A_j is the area of P_j. A conservative error bound ($C\,E\,B$) on the form factor in L_∞ norm can be obtained by bounding the difference between the maximum and minimum values of the form factor.[5] That is, we have that

$$\|F_{ij} - \hat{F}_{ij}\|_\infty \leq (\lceil k \rceil_{P_i,P_j} \cdot A_j - \lfloor k \rfloor_{P_i,P_j} \cdot A_j)$$

holds.

However, such an error bound will produce many unnecessary links and cause too much computational cost for the hierarchical radiosity algorithm to meet the user-specified error tolerance. Therefore the development of a tighter error bound is needed.[7,17]

We define the *middle value* of a function f over the domain $A \times B$ as

$$[f]_{A,B} \equiv \frac{1}{2}\left(\max_{x \in A, y \in B} f(x,y) + \min_{x \in A, y \in B} f(x,y)\right)$$

The approximate form factor $\tilde{F}_{ij}$ is given by

$$\begin{aligned}\tilde{F}_{ij} &= \int_{y\in P_j} [k]_{P_i,P_j}\mathrm{d}y \\ &= \int_{y\in P_j} \frac{1}{2}\left(\lceil k\rceil_{P_i,P_j} + \lfloor k\rfloor_{P_i,P_j}\right)\mathrm{d}y \\ &= \frac{1}{2}\left(\lceil k\rceil_{P_i,P_j}\cdot A_j + \lfloor k\rfloor_{P_i,P_j}\cdot A_j\right)\end{aligned}$$

We can derive a tighter error bound (TEB) on the form factor in L_∞ norm as

$$\begin{aligned}\|F_{ij} - \tilde{F}_{ij}\|_\infty &= \left\|\left(\int_{y\in P_j} k(x,y)\mathrm{d}y - \int_{y\in P_j}[k]_{P_i,P_j}\mathrm{d}y\right)\right\|_\infty \\ &= \left\|\int_{y\in P_j}\left(k(x,y) - \frac{\lceil k\rceil_{P_i,P_j} + \lfloor k\rfloor_{P_i,P_j}}{2}\right)\mathrm{d}y\right\|_\infty \\ &= \max_{x\in P_i}\left|\int_{y\in P_j}\left(k(x,y) - \frac{\lceil k\rceil_{P_i,P_j} + \lfloor k\rfloor_{P_i,P_j}}{2}\right)\mathrm{d}y\right| \\ &\le \int_{y\in P_j}\frac{\lceil k\rfloor_{P_i,P_j} - \lfloor k\rfloor_{P_i,P_j}}{2}\,\mathrm{d}y \\ &= \frac{1}{2}\left(\lceil k\rceil_{P_i,P_j}\cdot A_j - \lfloor k\rfloor_{P_i,P_j}\cdot A_j\right)\end{aligned}$$

This error bound depends strongly on the value of $\tilde{F}_{ij}$ and is tighter than the CEB.

3. A WEIGHTED ERROR METRIC

The shadow plays an important role in determining the human perception of image quality. In this section we propose a weighted error metric in form factor computation such that more effort is automatically applied to shadow boundaries.

3.1. Shadows

An area light source casting light onto an object will result in a shadow consisting of the penumbra and the umbra. The penumbra is the area receiving part of the light from the area light source, while the umbra is the region receiving no light from the area light source directly. Consider Figure 1. Point x_1, unable to perceive the area light source, is in the umbra. Point x_2, perceiving part of the area light source, is in the penumbra. Point x_3, perceiving the entire area light source, is not in the shadow. Therefore whether a point is in the region of shadow or not depends on its visibility from the area light source. An inaccurate calculation of the visibility will cause errors in the shadow.

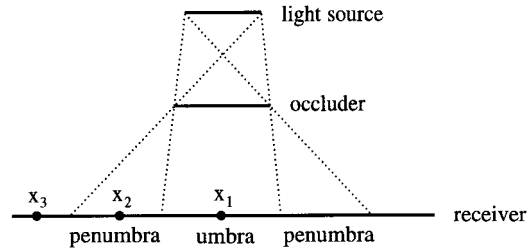

Figure 1. The visibility from a point to an area light source

3.2. Visibility error

The visibility error[9] of a point x illuminated by an area light source S can be obtained as follows. Let $V_x(y)$ be the visibility function, where y is a point on light source S, and $\overline{V_x}$ be its average visibility. For a point x illuminated by S, the visibility errors measured by L_1 and L_2 norms are given by

$$\begin{aligned}
\|V_x - \overline{V_x}\|_1 &= \frac{1}{A}\int_{y\in S} |V_x(y) - \overline{V_x}|\, dy \\
&= \frac{1}{A}\left(\int_{y\in S_{\text{vis}}} |1 - \overline{V_x}|\, dy + \int_{y\in S-S_{\text{vis}}} |0 - \overline{V_x}|\, dy\right) \\
&= \frac{1}{A}\left((1 - \overline{V_x})\int_{y\in S_{\text{vis}}} dy + \overline{V_x}\int_{y\in S-S_{\text{vis}}} dy\right) \\
&= \frac{1}{A}\left[(1 - \overline{V_x})A\overline{V_x} + \overline{V_x}A(1 - \overline{V_x})\right] \\
&= 2\overline{V_x}(1 - \overline{V_x})
\end{aligned}$$

and

$$\begin{aligned}
\|V_x - \overline{V_x}\|_2 &= \left(\frac{1}{A}\int_{y\in S} |V_x(y) - \overline{V_x}|^2\, dy\right)^{\frac{1}{2}} \\
&= \left[\frac{1}{A}\left(\int_{y\in S_{\text{vis}}} |1 - \overline{V_x}|^2\, dy + \int_{y\in S-S_{\text{vis}}} |0 - \overline{V_x}|^2\, dy\right)\right]^{\frac{1}{2}} \\
&= \left[\frac{1}{A}\left((1 - \overline{V_x})^2\int_{y\in S_{\text{vis}}} dy + \overline{V_x}^2\int_{y\in S-S_{\text{vis}}} dy\right)\right]^{\frac{1}{2}} \\
&= \left(\frac{1}{A}\left[(1 - \overline{V_x})^2 A\overline{V_x} + \overline{V_x}^2 A(1 - \overline{V_x})\right]\right)^{\frac{1}{2}} \\
&= [\overline{V_x}(1 - \overline{V_x})]^{\frac{1}{2}}
\end{aligned}$$

respectively, where A is the area of S, S_{vis} is the region of S that is visible from x, and $S - S_{\text{vis}}$ depicts the region of S that is invisible from x. Hence both estimates reveal that the error on visibility for a point illuminated by an area light source is dependent on the term $\overline{V_x}(1 - \overline{V_x})$. Consequently, a partially visible case leads to an error. Radiosity of the penumbra region needs more accurate computation to achieve realistic images.

3.3. A weighted error metric based on visibility

We define a weight for each point in three-dimensional space. When radiosities are evaluated, much emphasis is put on regions with higher weights to achieve more accurate solutions.

From the discussion in Section 3.2 the weight of a point in the penumbra is set to be greater than one and proportional to its visibility error. This implies that radiosities of points in the penumbra are computed with a higher degree of precision. Also, for the points outside the penumbra, their weights are kept at one. This means that radiosities of points outside the penumbra are calculated normally. By applying the visibility error of a point illuminated by an area light source S, as shown in Figure 2, a weighting function $W(x)$ can be defined as

$$W(x) = T\overline{V_x}(1 - \overline{V_x}) + 1, \quad 0 \le \overline{V_x} \le 1$$

where the parameter T is a positive number that scales the range of the weighting function. Note that if there are two or more area light souces, the weight of a point can be obtained by first computing a weight of the point from each area light source and then finding the maximum one among them.

From the above discussion the *weighted error metric* in p-norm is defined as

$$\|F_{ij} - \tilde{F}_{ij}\|_p^{\mathrm{w}} \equiv \|(F_{ij} - \tilde{F}_{ij})W\|_p = \left(\int |(F_{ij} - \tilde{F}_{ij})W|^p \, \mathrm{d}x\right)^{1/p}$$

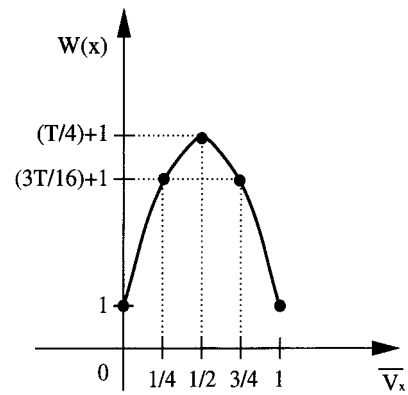

Figure 2. The weighting function W(x)

We can use the concept discussed in Section 2 to derive an error bound on the weighted error metric as a subdivision criterion for the hierarchical radiosity algorithm. To compare the *C E B*, we will use the ∞-norm in the rest of this paper. A conservative error bound (*C E B W*) on the weighted error metric in ∞-norm can be obtained as

$$\begin{aligned}\|F_{ij} - \tilde{F}_{ij}\|_{\infty}^{w} &\equiv \|(F_{ij} - \tilde{F}_{ij})W\|_{\infty} \\ &= \max_{x \in P_i} |(F_{ij} - \tilde{F}_{ij})W| \\ &\leq \max_{x \in P_i} |(F_{ij} - \tilde{F}_{ij})| \cdot \max_{x \in P_i} |W| \\ &\leq (\lceil k \rceil_{P_i,P_j} \cdot A_j - \lfloor k \rfloor_{P_i,P_j} \cdot A_j) \cdot \lceil W \rceil_{P_i,S}\end{aligned}$$

Besides, a tighter error bound (*T E B W*) on the weighted error metric in ∞-norm can be obtained as

$$\|F_{ij} - \tilde{F}_{ij}\|_{\infty}^{w} \leq \frac{1}{2}(\lceil k \rceil_{P_i,P_j} \cdot A_j - \lfloor k \rfloor_{P_i,P_j} \cdot A_j) \cdot \lceil W \rceil_{P_i,S}$$

4. ANALYSIS AND COMPARISON

We compare the hierarchical radiosity algorithm[2] using the *T E B*, *C E B W* and *T E B W* with that using the *C E B*. All experiments are implemented on an SGI workstation with 200 MHz R4400 CPU. We use the point-sampling-based technique[5] to calculate form factor bounds and the upper bound of the weighting function. In our implementation we use 16 samples for each pair of patches. The assignment of the parameter *T* in the weighting function depends on the desired accuracy of the penumbra and the given environment. In our implementation we select 25, 35 and 45 for *T*. We use the RMS error to measure the quality of the radiosity solutions of penumbra regions by using a 64×64 mesh on the receiver (floor). The reference solution is obtained by the hierarchical radiosity algorithm using the *C E B* with a very high precision (the user-specified error tolerance $F_{\text{eps}} = 10^{-5}$).

First, as shown in Figure 3, we construct two simple test environments to compare the links produced by the hierarchical radiosity algorithm using the *C E B* and the

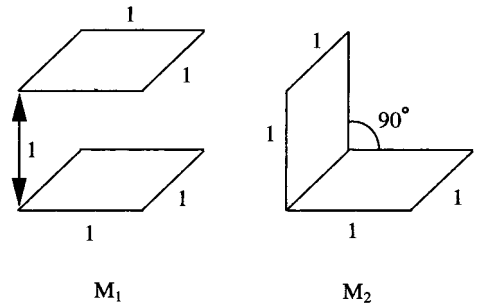

Figure 3. Simple test environments

Table I. Test results of M_1 (parallel case)

F_{eps}	Links		Reduction rate (%)
	CEB	*TEB*	
0·005	4096	3796	7·3
0·006	4096	3196	22·0
0·007	4096	2956	27·8
0·008	4036	2956	26·8
0·009	4036	1756	56·5
0·010	3796	256	93·3

T E B. The left environment, M_1, consists of two parallel unit squares, one unit distance apart. The right one, M_2, is composed of two perpendicular unit squares. The results are given in Tables I and II. For the 'parallel' case the variance of the form factor values is small. When F_{eps} is small, the reduction rate is low. For instance, when F_{eps} is 0·005, the reduction rate is only 7·3 per cent. This fact implies that most estimated error bounds are much larger than the given error tolerance and cause more subdivisions. When F_{eps} is large, the reduction rate is higher. For instance, when F_{eps} is 0·010, the reduction rate is 93·3 per cent. This fact means that most estimated error bounds are much smaller than the given error tolerance and cause fewer subdivisions. For the 'perpendicular' case the variance of the form factor values is larger. The reduction rate is about 50 per cent for any value of F_{eps}, as depicted in Table II.

As noted by Smits *et al.*,[5] the computation of the lower bound on visibility is a very expensive process. Therefore in the following experiments the lower bound on the form factor is set to zero.

Next we construct a simple environment, M_3, containing an area light source, an occluder and a receiver in distinct parallel planes to compare the accuracy of shadow boundaries of the hierarchical radiosity algorithm using the *C E B* and the *C E B W*. Table III gives the results for two different user-specified error tolerances. As the table shows, the RMS error obtained by the hierarchical radiosity algorithm using the *C E B W* is smaller than that obtained by the hierarchical radiosity algorithm using the *C E B*. These results mean that the hierarchical radiosity algorithm using

Table II. Test results of M_2 (perpendicular case)

F_{eps}	Links		Reduction rate (%)
	CEB	*TEB*	
0·005	14416	6976	51·6
0·006	11656	5836	49·9
0·007	10516	5656	46·2
0·008	9046	4246	53·1
0·009	8296	3676	44·3
0·010	6976	3256	53·3

Table III. Test results of M_3: RMS error ($\times 10^{-4}$)

F_{eps}	*CEB*	*CEBW*		
		$T = 25$	$T = 35$	$T = 45$
0·015	276	145	130	87
0·010	216	69	52	49

Table IV. Test results of M_4 for $F_{eps} = 0{\cdot}015$

	CEB	*TEBW*		
		$T = 25$	$T = 35$	$T = 45$
Time (s)	291	221	235	247
Links	112612	70237	75874	81709
RMS error ($\times 10^{-7}$)	7327	4738	2021	1641

the *C E B W* increases the accuracy along shadow boundaries in comparison with the hierarchical radiosity algorithm using the *C E B*. To compare the visual accuracy along shadow boundaries, in Plates 1 and 2 we show the results obtained by the hierarchical radiosity algorithm using the *C E B* and the *C E B W* for $T = 45$ ($F_{eps} = 0{\cdot}015$). As the images show, the hierarchical radiosity algorithm using the *C E B W* can generate a better visual result on shadow boundaries.

Then we construct an environment, M_4, that is a room containing a chair and an area light source (104 input surfaces) to compare the performance, the links produced and the accuracy of shadow boundaries of the hierarchical radiosity algorithm using the *C E B* and the *T E B W*. The experimental results are given in Tables IV and V. The computation time of the hierarchical radiosity algorithm using the *T E B W* is less than that of the hierarchical radiosity algorithm using the *C E B*. The number of links produced by the hierarchical radiosity algorithm using the *T E B W* is smaller than that produced by the hierarchical radiosity algorithm using the *C E B*. The RMS error of the hierarchical radiosity algorithm using the *T E B W* is smaller than that

Table V. Test results of M_4 for $F_{eps} = 0{\cdot}010$

	CEB	*TEBW*		
		$T = 25$	$T = 35$	$T = 45$
Time (s)	406	314	340	376
Links	180421	109246	123928	143293
RMS error ($\times 10^{-7}$)	7322	1732	917	650

of the hierarchical radiosity algorithm using the *C E B*. These results mean that the hierarchical radiosity algorithm using the *T E B W* not only improves the performance but also increases the accuracy of shadow boundaries in comparison with the hierarchical radiosity algorithm using the *C E B*. Hence we can get an efficient hierarchical radiosity algorithm capable of enhancing the accuracy along shadow boundaries. To compare the visual accuracy along shadow boundaries, in Plates 3 and 4 we show the radiosity solutions obtained by the hierarchical radiosity algorithm using the *C E B* and the *T E B W* for $T = 45$ ($F_{\text{eps}} = 0{\cdot}010$). As the images show, the hierarchical radiosity algorithm using the *T E B W* can generate a better representation along shadow boundaries.

Finally we apply the hierarchical radiosity algorithm using the *T E B W* to an environment containing 938 input surfaces. The user-specified error tolerance is set to 0·01 and the parameter *T* is set to 45. It takes about 162 min and creates 640,709 links on the hierarchy for the radiosity solution. Plate 5 depicts the resulting image.

5. CONCLUSIONS AND FUTURE WORK

We derive a tighter error bound on form factors as a subdivision criterion for the hierarchical radiosity algorithm. Such an error bound can reduce many unnecessary links and improve the performance of the hierarchical radiosity algorithm to meet a user-specified error tolerance. Moreover, we propose a weighted error metric based on the visibility for radiosity. Our method properly puts stress on aspects of shadow boundaries. Using the tighter error bound on the weighted error metric, we not only improve the performance but also enhance the accuracy along shadow boundaries of the hierarchical radiosity algorithm.

Several problems need further research. First, we will make an in-depth study on deriving tighter error bounds on form factors. Next, the weighting function is based on the visibility error for a point illuminated by an area light source. A more in-depth study should be made of the weighting function to construct better weighted error metrics for radiosity. Finally, the development of perceptually based error metrics for image synthesis is necessary, since the complete simulation of a global illumination model should consider the perception of observers.[18] We will also consider an image's perception to derive more accurate error metrics for image synthesis.

Acknowledgements

This work was supported partially by the National Science Council, Republic of China, under grant NSC86–2745–E009–002. We would like to thank reviewers for their helpful suggestions.

REFERENCES

1. M. F. Cohen, D. P. Greenberg, D. S. Immel and P. J. Brock, 'An efficient radiosity approach for realistic image synthesis', *IEEE Computer Graphics and Applications*, **6**(3), 26–35 (1986).
2. P. Hanrahan, D. Salzman and L. Aupperle, 'A rapid hierarchical radiosity algorithm', *Computer Graphics*, **25**(4), 197–206 (1991).
3. A. A. Appel, 'An efficient program for many-body simulation', *SIAM Journal on Scientific & Statistical Computing*, **6**(1), 85–103 (1985).
4. B. E. Smits, J. R. Arvo and D. H. Salesin, 'An importance-driven radiosity algorithm', *Computer Graphics*, **26**(2), 273–282 (1992).

5. B. Smits, J. Arvo and D. Greenberg, 'A clustering algorithm for radiosity in complexity environments', *Proceedings of ACM SIGGRAPH '94*, 1994, pp. 435–442.
6. J. Arvo, K. Torrance and B. Smits, 'A framework for the analysis of error in global illumination algorithms', *Proceedings of ACM SIGGRAPH '94*, 1994, pp. 75–84.
7. D. Lischinski, B. Smits and D. P. Greenberg, 'Bounds and error estimates for radiosity', *Proceedings of ACM SIGGRAPH '94*, 1994, pp. 67–74.
8. M. Pellegrini, 'Monte Carlo approximation of form factors with error bounded a priori', *Proceedings of the Eleventh Annual ACM Symposium on Computational Geometry*, 1995, pp. 287–296.
9. F. Sillion and G. Drettakis, 'Feature-based control of visibility error: a multi-resolution clustering algorithm for global illumination', *Proceedings of ACM SIGGRAPH '95*, 1995, pp. 145–152.
10. P. R. Atherton, K. Weiler and D. P. Greenberg, 'Polygon shadow generation', *Computer Graphics*, **12** (3), 275–281 (1978).
11. N. Chin and S. Feiner, 'Near real-time shadow generation using BSP trees', *Computer Graphics*, **23**(3), 99–106 (1989).
12. N. Chin and S. Feiner, 'Fast object-precision shadow generation for area light sources using BSP trees', *Proceedings of the 1992 Symposium on Interactive 3D Graphics*, 1992, pp. 21–30.
13. F. C. Crow, 'Shadow algorithms for computer graphics', *Computer Graphics*, **11**(2), 242–248 (1977).
14. T. Nishita and E. Nakamae, 'Continuous tone representation of three-dimensional objects taking account of shadows and interreflection', *Computer Graphics*, **19**(3), 23–30 (1985).
15. J. Stewart and S. Ghali, 'Fast computation of shadow boundaries using spatial coherence and backprojections', *Proceedings of ACM SIGGRAPH '94*, 1994, pp. 231–238.
16. A. Watt and M. Watt, *Advanced Animation and Rendering Techniques Theory and Practice*, Addison-Wesley, Reading, MA, 1992.
17. C. C. Chang and Z. C. Shih, 'Tighter error bounds on form factors for hierarchical radiosity', *Proceedings of the Fourth Pacific Conference on Computer Graphics and Applications, Pacific Graphics '96*, 1996, pp. 147–158.
18. M. F. Cohen and J. R. Wallace, *Radiosity and Realistic Image Synthesis*, Academic, New York, 1993.

